

Interaction of Singapore and Johor Bahru on Urban Climate during Monsoon Seasons

Jochen Kraus¹, Andhang Rakhmat Trihamdani², Tetsu Kubota², Han Son Lee³, Kensuke Kawamura²

1 Institute for Systems Sciences, Innovation and Sustainability Research, Merangasse 18/1, A-8010 Graz, jochen.kraus@edu.uni-graz.at

2 Graduate School for International Development and Cooperation, 1-5-1 Kagamiyama, Higashi-Hiroshima 739-8529, Japan, andhang.rt@gmail.com, tetsu@hiroshima-u.ac.jp, kamuken@hiroshima-u.ac.jp

3 Graduate School of Science and Engineering, Saitama University, Japan, hslee@mail.saitama-u.ac.jp

dated : 30 June 2015

1. Introduction

Urban development in rapidly urbanizing regions, such as Southeast Asia, requires comprehensive planning and consideration of local characteristics. Tropical and subtropical cities, with their high temperatures and humidity, are particularly affected by increasing air temperature in relatively densely built-up areas. Increase in air temperature is in turn associated with higher cooling loads and hence higher energy consumption (Santamouris et al., 2001). Many major cities developed therefore strategies to ensure sustainable urban development. However, in regard to urban climate, proposed development strategies are limited to the borders of the city or the country. A comprehensive understanding of interactions between two major cities on their urban climate needs further investigation.

This study aims to assess the interaction between the development in Singapore and Johor Bahru on urban climate and formation of Urban Heat Island (UHI). Despite relatively low wind speed, the characteristic wind flow pattern in this region is expected to impact the occurrence of UHIs in Singapore and Johor Bahru and provide some understanding on cross-boundary mitigation strategies.

Johor Bahru is located in the southern-most tip of Peninsular Malaysia and is the second largest city after Kuala Lumpur. Singapore is a city-state, located on an island south of Johor Bahru. Both cities are separated by the Strait of Johor (see figure 1). Recently, Johor Bahru is experiencing rapid development in the course of the implementation of the Comprehensive Development Plan (CDP) 2006. The CDP proposes strategic interventions to promote economic growth and improve quality of life in South Johor. Singapore, in contrast, almost reached its physical limits for further development. By 2030, Singapore will develop about 7.3% of land to meet its future land requirements.

The wind flow over Peninsular Malaysia is determined by southwest and northeast monsoon, and by intermonsoon seasons. From June to September, southwesterly winds prevail, whereas from November to March the prevailing wind direction is northeast. In the intermonsoon season, wind flow is light and variable. Uniform and periodic changes of wind flow during summer and winter were of particular interest for this study.

2. Methodology

The assessment of monsoon interaction between the two major cities was conducted using the Weather Research and Forecasting (WRF) model (version 3.6.1) with integrated Advanced Research WRF (ARW) dynamics solver (Skamarock et al., 2008). WRF is a numerical model which integrates various components to provide operation forecast and simulate atmospheric conditions on the mesoscale. The grid cell resolution was chosen as 0.5 km which utilizes the maximum capability of the model to simulate atmospheric conditions and sufficiently represents the urban layer. WRF modeling was performed in an interactive grid nesting with four computational domains (domain 1-4) with resolution of 13.5 km, 4.5 km, 1.5 km, and 0.5 km, respectively. The vertical resolution comprised of 30 layers which extended to 50 hPa. The initial and lateral boundary conditions were defined using data from National Centers for Environmental Prediction (NCEP). The NCEP FNL (Final) data were also used as Four-dimensional Data Assimilation (FDDA) in all four domains. Table 1 lists all schemes applied in the WRF model.

Table 1: WRF modeling schemes

| Parameter | Scheme | Reference |
|---------------------|---------------------------------|-------------------------|
| Longwave Radiation | RRTM Scheme | Mlawer et al., 1997 |
| Shortwave Radiation | Dudhia Scheme | Dudhia, 1989 |
| Surface Layer | Monin-Obukhov Similarity Scheme | Monin and Obukhov, 1954 |
| Land-Surface | Noah LSM | Tewari et al., 2004 |

| | | |
|--------------|-----------------------|------------------------------|
| PBL Type | YSU | Hong, Noh, and Dudhia, 2006 |
| Microphysics | WRF SM 3-class scheme | Hong, Dudhia, and Chen, 2004 |
| Cumulus | Kain-Fritsch Scheme | Kain, 2004 |

The main input data for WRF consist of terrestrial and climate data. Apart from default terrestrial data, which are represented by the USGS Global Land Cover Characteristics (GLCC) data (Loveland et al., 2010) for domain 1 and 2, this research utilizes Global Land Cover by National Mapping Organizations (GLCNMO)(versions 1)(see Tateishi, Uriyangqai, et al., 2011) for domain 3, and current terrestrial data produced by utilizing Landsat-8 imagery and supervised classification method for domain 4. WRF modeling accuracy strongly depends on the available data on land use and land cover (LULC). Therefore, the preparation LULC data that represent the current development in JB and Singapore in the first step of this study played a vital role.

The preparation of LULC data was based on the spatial and spectral information retrieved from Landsat-8 imagery acquired on 18 June, 2013 (scene 1) and 27 June, 2013 (scene 2). Scene 1 consists of the western coast of Peninsular Malaysia in the north, the Strait of Malacca in the centre, and several islands belonging to Sumatra (Indonesia) in the south of the image. Scene 2 comprises of the southern-most tip of Peninsular Malaysia and Singapore Island in the centre, Batam, Bintan, and several other Indonesian islands in the south, and the South China Sea in the east of the image. High incidence of clouds strongly affected several areas in scene 1 and 2 that were vital for the preparation of the LULC map. Thus, Landsat-8 imagery from 22 February, 2013 and 24 April, 2013 were used to account for cloud contamination in the southern-most tip of Kota Tinggi district, southern and south-eastern part of Singapore.

The observational climate data were obtained from weather stations in Senai International Airport, Johor Bahru as well as from four weather stations in Singapore located in Changi, Seletar, Paya Lebar, and on the campus of the National University of Singapore (NUS)(see figure 2). The climate data for all weather stations except at NUS were provided by the National Climate Data Center of the National Oceanic and Atmospheric Administration (NOAA).

Simulation periods were chosen to represent the southwest and northeast monsoon season for a typical month. Typical month was defined as the month in which the mean temperature is closest to the 13-year mean value. For the southwest monsoon, the simulation period was from 9 June to 15 June, 2009. The mean air temperature in this period was 27.46 °C. The prevailing wind direction is south. However, at night, the prevailing wind direction significantly changes and with wind blowing from the north. The simulation period for the northeast monsoon was 3 February to 9 February, 2009. The mean air temperature during this period was 25.93 °C with prevailing wind direction from north-northeast. There were no differences between day and night conditions.

3. Results and Discussion of Urban Climate Modeling

3.1 Model Validation

WRF modeling depends mainly on the terrestrial and climate input data. The assessment of classification accuracy shall provide means to validate the prepared land cover data using supervised classification algorithm. The overall accuracy for the first Landsat-8 imagery resulted in 83.33%. In case of the second scene, the over accuracy was 87.40%. The prepared land cover data for domain 4 in WRF model accurately represent the actual land cover conditions and are sufficient to conduct simulations of SW- and NE-monsoon conditions (see figure 1).

The WRF model was validated using climate data from five weather stations (WSs). The validation was carried out for the period from 08:00 MYT (00:00 UTC) 12 to 08:00 MYT (00:00 UTC) 19 June, 2013. Table 2 summarizes the validation results. The deviation of simulated results from observed data occurs due to application of various schemes and input data that may affect the computational processes during the simulation.

The validation results for air temperature show correlation coefficient values (R^2) between 0.57 and 0.89. The variance between computed and observed values for WSs Senai, Changi, Seletar, and Paya Lebar can be sufficiently described by the linear fit of the WRF model. The geographic location of WS NUS at the southern coast of Singapore Island and hence the resulting impact of sea breeze on the measurement of air temperature may lead some inaccuracy in simulating the conditions on the small scale. Moreover, the campus of the NUS is characterized by wide green areas which may have additional effect on the measurement of air temperature. The RMSE for the air temperature ranges between 0.60 °C and 3.03 °C with the lowest value computed for WS NUS and the highest values for WS Paya Lebar.

The validation of wind speed results in overall lower correlation coefficients than for the air temperature. The R^2 values ranges between 0.48 and 0.64. The RMSE values are with 2.48 ms^{-1} highest for WS Senai and lowest for WS NUS (1.00 ms^{-1}). The simulation results of wind direction correspond well with the observed data at WS Senai, NUS, Seletar, and Changi. In case of WS Paya Lebar, the wind direction is slightly different from observed data. In particular wind speed and wind direction observed at urban sites are greatly influenced by urban morphology. Validation of simulation results with observed wind speed and wind direction data in the CBD, commercial or residential areas may differ from validation results presented in table 2.

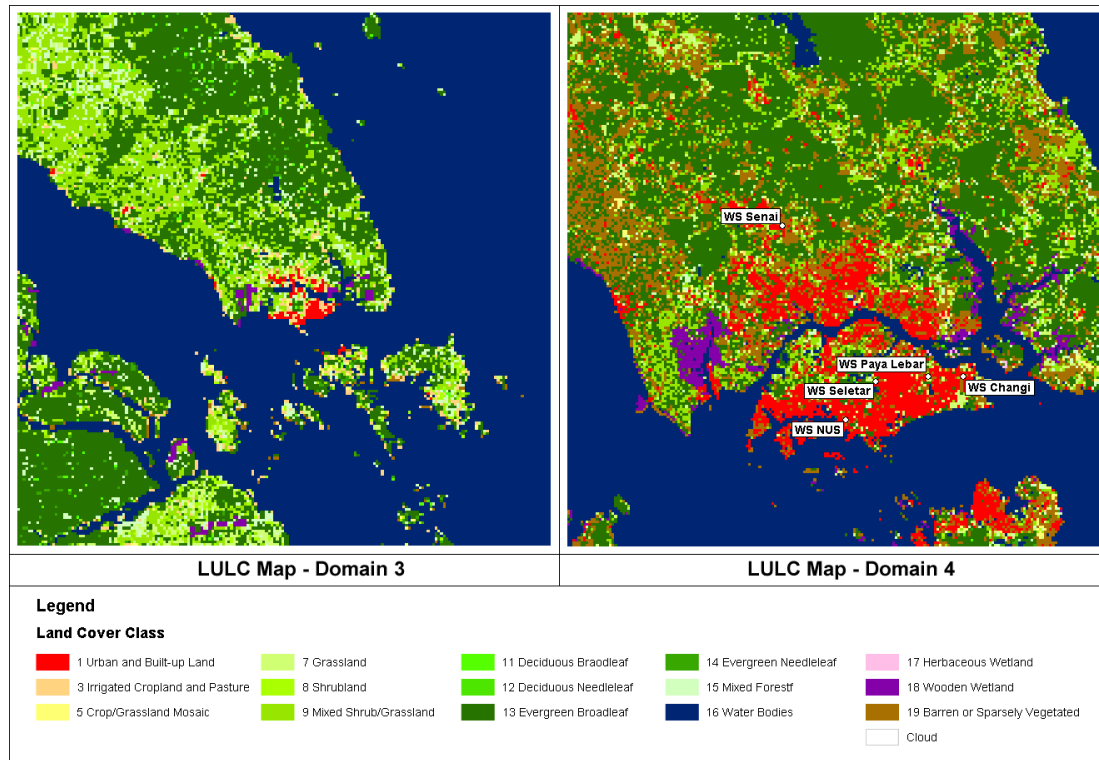


Figure 1: Land use and land cover map for domain 3 and domain 4

Table 2: Validation of WRF model

| | | Senai | Changi | Seletar | Paya Lebar | NUS |
|-------------|----------------|--------|--------|---------|------------|--------|
| Temperature | R ² | 0.892 | 0.734 | 0.863 | 0.821 | 0.570 |
| | RMSE | 1.274 | 1.143 | 1.561 | 3.032 | 0.599 |
| | Bias | -0.189 | -0.324 | -0.878 | -1.524 | 0.136 |
| Wind Speed | R ² | 0.643 | 0.483 | 0.542 | 0.548 | 0.540 |
| | RMSE | 2.482 | 1.775 | 1.731 | 1.390 | 1.007 |
| | Bias | 1.303 | 0.824 | 0.857 | 0.489 | -0.062 |

3.2 Simulation Results

The simulation results show an impact of prevailing wind direction during the respective monsoon season on the air temperature. In general, the hottest air temperature can be observed during the southwest monsoon. With sunrise, the air temperature rapidly increases to reach its maximum values around 2:00 pm or 3:00 pm. After the daily maximum, the air temperature begins to decrease to reach its minimum values around sunrise (7:00 am). The mean air temperature in the CBD of JB (designated as CBD_JB) is 29.46 °C whereas in the CBD of Singapore (designated as CBD_SNG) the mean air temperature is slightly lower (29.30 °C). During the northeast monsoon, the mean air temperature at CBD_SNG is higher than the mean air temperature at CBD_JB (27.45 vs. 26.89 °C). The wind speed ranges between 1.2 ms⁻¹ and 4.0 ms⁻¹ with a mean wind speed of around 2.4 ms⁻¹ during the SW-monsoon. During the NE-monsoon, the wind speed is generally higher ranging between 2.7 ms⁻¹ and 5.7 ms⁻¹. Table 3 summarizes all simulation results for JB and Singapore.

Table 3: Mean values of simulation results for JB and Singapore

| | CBD_JB | CBD_SNG | RES_JB | RES_SNG | RUR_Ave_JB | RUR_SNG |
|-----------------------------------|--------|---------|--------|---------|------------|---------|
| Temperature (in °C) | | | | | | |
| SW-Monsoon | 29.46 | 29.30 | 29.60 | 29.40 | 27.76 | 28.54 |
| NE-Monsoon | 26.89 | 27.41 | 26.71 | 26.83 | 25.29 | 26.47 |
| Wind Speed (in ms ⁻¹) | | | | | | |
| SW-Monsoon | 2.60 | 2.39 | 2.51 | 2.36 | 2.58 | 2.25 |
| NE-Monsoon | 4.19 | 4.01 | 3.89 | 4.52 | 4.16 | 3.86 |
| Relative Humidity (in %) | | | | | | |
| SW-Monsoon | 72.49 | 74.74 | 70.85 | 73.02 | 81.42 | 77.96 |
| NE-Monsoon | 73.62 | 70.93 | 74.42 | 75.41 | 82.29 | 76.27 |

JB = Johor Bahru; SNG = Singapore; CBD = Central Business District; RES = Residential Area; RUR = Rural Area

In case of JB, the mean UHI intensity can be calculated as 1.71 °C. The maximum mean UHI intensity of 2.43 °C is reached around 8:00 pm. The minimum mean UHI intensity of 0.73 °C can be observed at 10:00 am. At night, the mean UHI intensity is up to 2.10 °C high and decreases during the day to 1.39 °C. In Singapore's case, the mean UHI intensity is significantly lower as compared to JB case. The mean UHI intensity is 0.75 °C. The

maximum value of 1.78 °C is reached at 4:00 am and the minimum value of -0.52 °C at 2:00 pm. The UHI over Singapore dissolves at around 10:00 am and forms again at around 6:00 pm. In this period, the CBD of Singapore remains cooler than the rural area that was used as reference location to determine the UHI intensity. As shown in figure 2 (a-d), the sea breeze impacts the temporal variation of air temperature in the CBD of Singapore during the SW-monsoon (compare figure 2 (b)). The air temperature during the daytime is lower in the CBD than in the rural area leading thus to negative UHI intensity. After sunset, the air temperature in the rural rapidly decreases resulting in reoccurrence of the UHI effect. Figure 3 shows the spatial distribution of peak mean air temperature and the occurrence of maximum UHI intensity during the SW- and NE-monsoon seasons.

The urban center of JB is blocked by Singapore Island from the southeasterly sea breeze. The cooling effect of the sea breeze can be observed along the entire south coast of Singapore Island (compare figure 4). The air temperature difference between CBD_JB and CBD_SNG on 12 June, 2009 at 6:00 MYT is up to 3 °C. The morphology of Singapore's southern coast, which mainly consists of a high rise building front, hinders the cool air to reach far into the hinterland of Singapore. The air temperature is thus higher at the northern coast of Singapore compare to the southern coast. Unlike CBD_JB, the southwestern region of JB is likely to be affected by the southwesterly sea breeze. The mean air temperature in the southwestern region of JB is simulated to be up to 2 °C lower than in the urban areas that are cut off from the sea breeze. Gedzelman et al. (2003) found that sea breezes over coastal urban areas modify the UHI pattern by delaying its formation, reducing intensity, and displacing its effect further inland. Formation of UHI in coastal urban areas prevents the sea breeze to move further inland but the cooling impact of the sea breeze at the coastal front is much higher due to transfer of relatively cool air and enhanced wind speed.

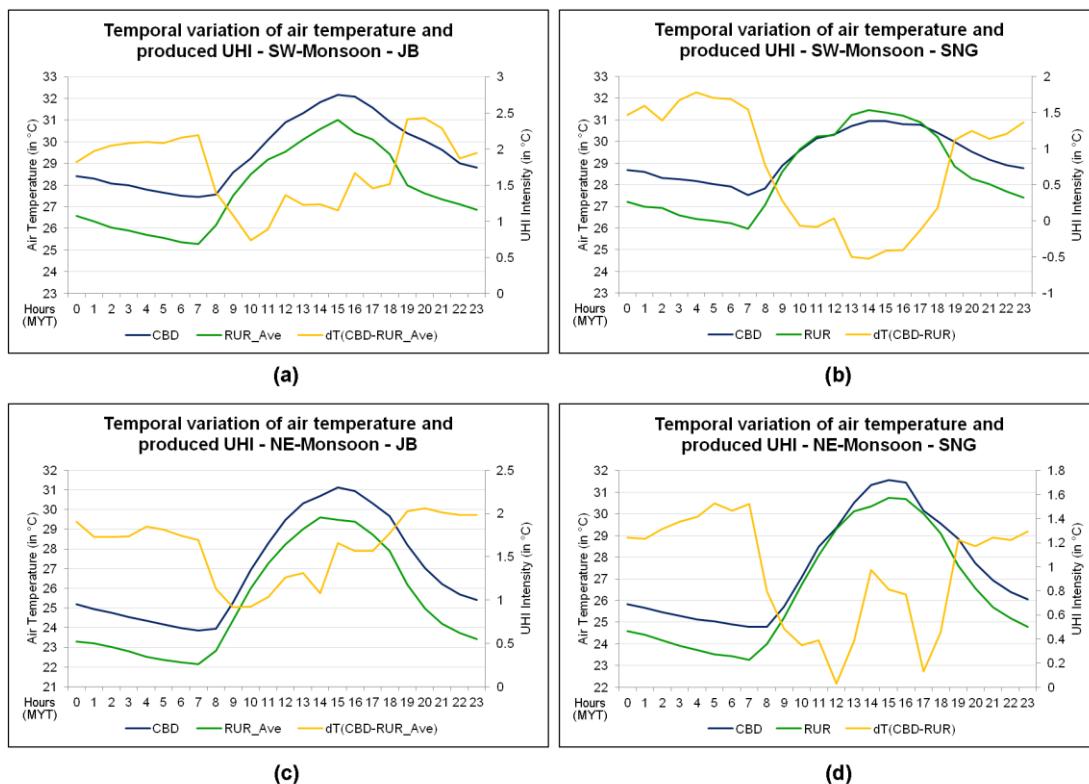


Figure 2: Temporal variation of urban and rural air temperature and produced UHI for monsoon seasons in JB and Singapore

As mentioned previously, during the SW-monsoon, the wind changes its direction by nearly 180° at night and blows from the north. The variation of wind direction is associated with extremely low wind speed of up to 0.20 ms⁻¹ and below. The air blowing from the north carries relatively warm air and results in higher air temperature along the southern coast of Singapore (see figure 4). The reversed wind direction impacts also the urban climate in JB. The cooler air from the rural areas north of the CBD_JB leads to lower air temperature in the northern part of JB. However, the air temperature difference between CBD_JB and CBD_SNG at night is small than during the daytime. Due to substantially lower wind speed, the cool air coming from the north does not affect the whole urban area on JB. The rural areas in the periphery of the city are largely affected by cool air. The cool air has this only limited effect on CBD_JB. The absorbed heat in the urban center, which is released as heat during the night, cannot be removed effectively by the low wind speed. As a consequence, the nocturnal mean UHI intensity is found to be highest during the SW-monsoon.

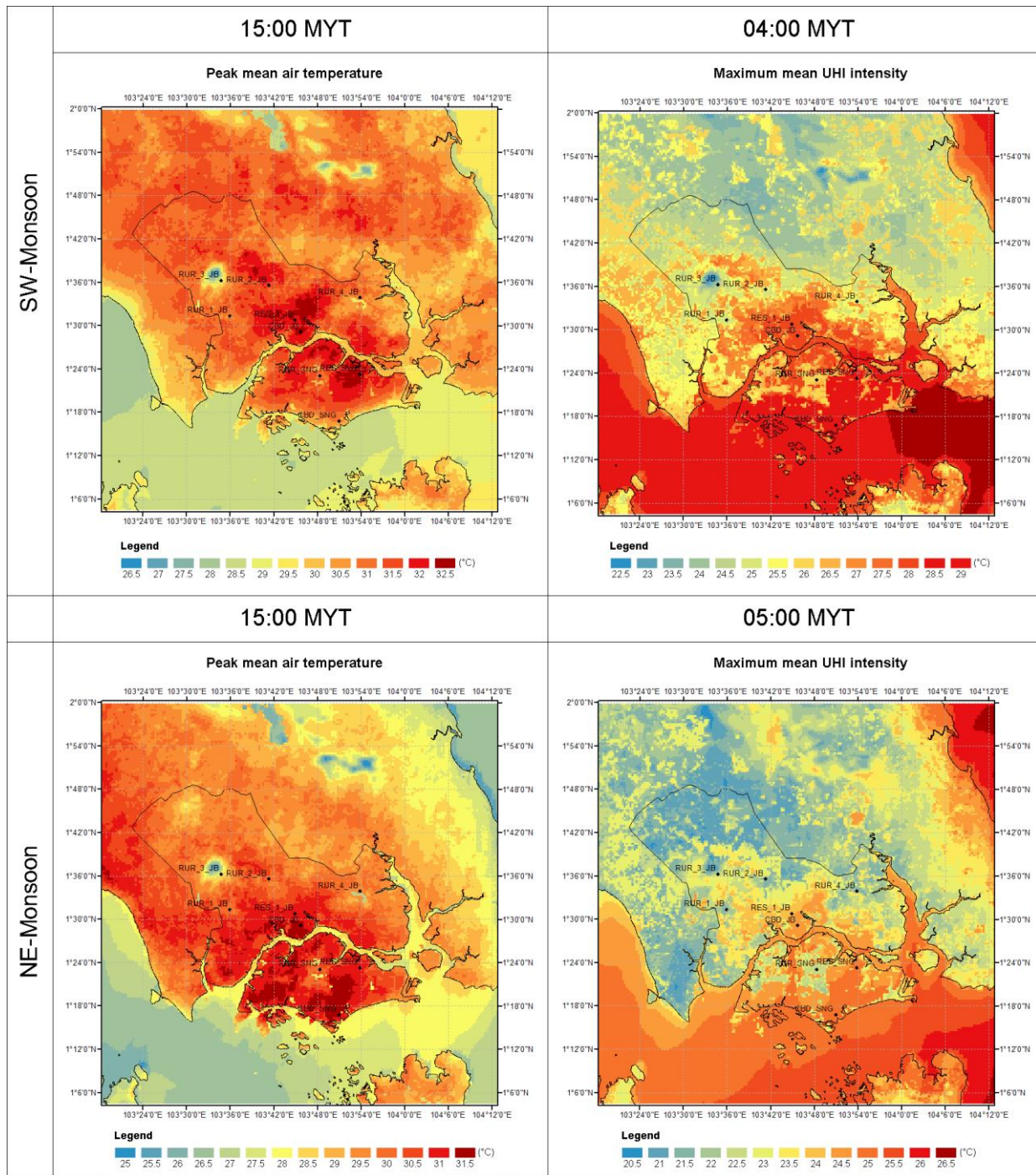


Figure 1: Peak mean air temperature and maximum mean UHI intensity in the monsoon seasons

4. Conclusion

The assessment of the current development in JB and Singapore shows an impact on the urban climate and UHI. Various factors including geographic location, seasonal wind changes, and urban morphology of both cities result in a unique constellation which affects the air temperature in the CBD of JB and Singapore. Despite a constant cool sea breeze during the SW-monsoon, cooler air temperature in the city center of JB cannot be observed. In case of Singapore, there is a clear indication of sea breeze effect that reduces the air temperature along the southern coast of Singapore below the values in rural areas. Comprehensive regional planning, including JB and Singapore may benefit future development of this metropolitan region by taking into account the building and street layout and the prevailing wind directions during the dominate monsoon seasons. Further research on the urban scale may results in findings that contribute to sustainable urban development of JB and Singapore.

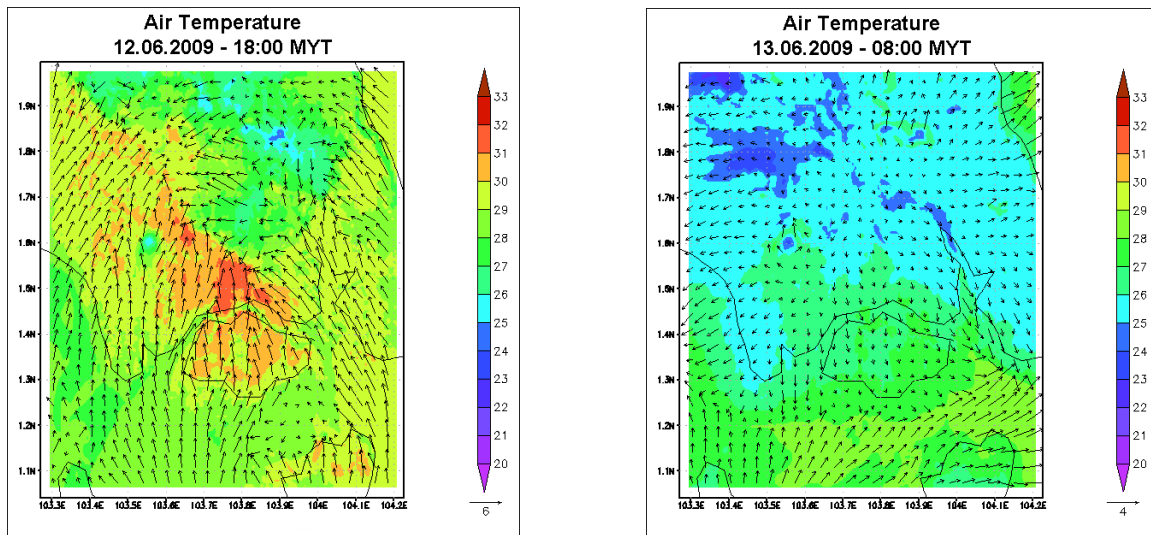


Figure 4: Air temperature and wind direction on 12 June, 2009 at 6:00 pm (left) and on 13 June, 2009 at 8:00 am (right)

References

- Dudhia, J., 1989: Numerical study of convection observed during the Winter Monsoon Experiment using a mesoscale two-dimensional model. *J. Atmo. Sci.* **46**, pp. 3077–3107.
- Gedzelman, S., Austin, S., Cermak, R., Stefano, N., Partridge, S., Quesenberry, S., and Robinson, D., 2003: Mesoscale aspects of the Urban Heat Island around New York City. *Theoretical and Applied Climatology*, **76**, pp. 29–42.
- Hong, S., Dudhia, J., and Chen, S., 2004: A revised approach to ice microphysical processes for the bulk parameterization of clouds and precipitation. *Monthly Weather Review*, **132**, pp. 103–120.
- Hong, S., Noh, Y., and Dudhia, J., 2006: A new vertical diffusion package with an explicit treatment of entrainment processes. *Monthly Weather Review*, **134**, pp. 2318–2341.
- Kain, J., 2004: The Kain-Fritsch convective parameterization: An update. *J. Climate Appl. Meteorol.* **43**, pp. 170–181.
- Loveland, T., Reed, B., Brown, J., Ohlen, D., Zhu, Z., Yang, L., and Merchant, J., 2010: Development of a global land cover characteristics database and IGBP DISCover from 1 km AVHRR data. *International Journal of Remote Sensing*, **21** (6-7), pp. 1303–1330.
- Mlawer, E., Steven, J., Taubman, J., Brown, P., Iacono, M., and Clough, S., 1997: Radiative transfer for inhomogeneous atmospheres: RRTM, a validated correlated-k model for the longwave. *Journal of Geophysical Research*, **102**, pp. 16663–16682.
- Monin, A. and Obukhov, A., 1954: Basic laws of turbulent mixing in the surface layer of the atmosphere. *Contrib Geophys Inst Acad Sci USSR*, **151**, pp. 163–187.
- Santamouris, M., Papanikolaou, N., Livada, I., Koronakis, I., Georgakis, C., Argiriou, A., and Assimakopoulos, D., 2001: On the impact of urban climate on the energy consumption of buildings. *Solar Energy*, **70** (3), pp. 201–216.
- Skamarock, W., Klemp, J., Dudhia, J., Gill, D., Barker, D., Duda, M., Huang, X., Wang, W., and Powers, J. 2008: A description of the Advanced Research WRF Version 3: NCAR Technical Note. Boulder.
- Tateishi, R., Uriyangqai, B., Al-Bilbisi, H., Ghar, M. A., Tsend-Ayush, J., Kobayashi, T., Kasimu, A., Hoan, N. T., Shalaby, A., Alsaadeh, B., Enkhzaya, T., Gegentana, and Sato, H. P., 2011: Production of global land cover data – GLCNMO. *International Journal of Digital Earth*, **4** (1), pp. 22–49.
- Tewari, M., Chen, W., Dudhia, J., LeMone, M., Mitchell, K., Ek, M., Gayno, G., Wegiel, B. J., and Cuenca, R., 2004: Implementation and verification of the unified NOAA land surface model in the WRF model. In *Proceedings of the 20th Conference on Weather Analysis and Forecasting/16th Conference on Numerical Weather Prediction*. Seattle.